Imaging and Radiation Research (2019) Volume 2 Issue 1
doi:10.24294/irr.v2i1.1716

REVIEW ARTICLE

Initial approach to mediastinal alterations: Review of their radiographic anatomical references

Emmanuel Salinas Miranda*, Luisa Karen Cifuentes, Juan Gonzalo Vélez, Bibiana Andrea Pinzón

Departamento de Radiología, Hospital universitario Fundación Santa Fe de Bogotá, Bogotá, DC, Colombia. E-mail: emmanuels7@gmail.com

ABSTRACT

The suspicion of mediastinal alterations, always includes in its initial study, the chest radiography. The identification of mediastinal alterations in the X-ray is a priority. The knowledge of the mediastinal references and the identification of their alterations allows the suspicion of a pathology specific to each of the mediastinal spaces. When the semiology of mediastinal lesions, their location and the three most frequent pathologies are taken into account, the possibility of having an etiological diagnosis increases[1]. This is a review article based on a detailed literature search, in which radiological mediastinal references are studied, with emphasis on the epidemiological data of each one of them.

Keywords: Epidemiology; Surgery; Radiography; Tumors; Evidence-based Medicine

ARTICLE INFO

Received: 1 April 2019
Accepted: 28 May 2019
Available online: 2 June 2019

1. Introduction

The mediastinum is an intrathoracic extra-pleural anatomical compartment, located in the center of the thorax, between both lungs, behind the sternum and the chondrocostal junctions and in front of the vertebral bodies and ribs. In its inferior aspect, it is limited by the diaphragm muscle, and in its superior aspect by the cervicothoracic strait.

In chest radiography, mediastinal landmarks may be the product of the continuity of mediastinal, pulmonary or vertebral structures when they are tangentially traversed by the x-ray beam or they may be a visual effect such as the Mach bands discussed later. These silhouettes can be divided into lines, bands or interfaces[1,2] (**Figure 1**).

The absence, thickening or displacement of one or more of the mediastinal lines, bands or interfaces may signify a mediastinal injury; however, the technical conditions of the radiograph and anatomical variations also modificate the frequency and the way in which these mediastinal silhouettes or their alterations are observed. The most frequently visualized lines are the paratracheal band and the paraspinal line on the right side[2]. The rest of the mediastinal landmarks are visualized in varying percentages in the chest radiograph (**Table 1**).

The first step in approaching mediastinal masses on chest radiography is to suspect their mediastinal origin. The radiographic features of a lesion that point to a mediastinal origin are: the intimate relationship of the mass with the mediastinal structures, smooth and sharp margins, and the formation of obtuse angles between the mass and the lung field[1,3] (**Figure 2**).

The intimate effect with mediastinal structures is infiere from the alteration and displacement of mediastinal structures adjacent to the lesion, such as the trachea, main bronchi or heart (**Figure 3**).

Chest radiograph shows a mass in the upper third of the thorax, showing an intimate effect with mediastinal structures. The mass is conditioned by displacement of the trachea. It has sharp, well-defined margins with obtuse angles. This patient has a histologic diagnosis of thyroid carcinoma.

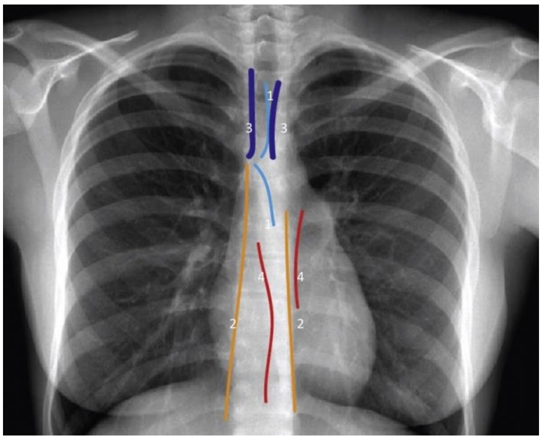

Figure 1. Chest X-ray scheme with lines, bands and interfaces. (1) Representation of superior-posterior and inferior-anterior junction lines; (2) paraspinal lines; (3) paratracheal bands; (3) azygo-aesophageal; (4) para-aortic interfaces.

Table 1. Frequency of visualization of the mediastinal lines, bands and interfaces

Anterior joint line	24%
Rear joint line	32%
Right paratracheal band	97%
Left paratracheal band	31%
Right paraspinal line	23%
Left paraspinal line	41%
Left para-aortic recess	40% ^
Aesophageal - esophageal interface	5%*
Aortopulmonary window	90%

* Biemans JM approximate calculation[4]; ^ Dobson MJ calculation

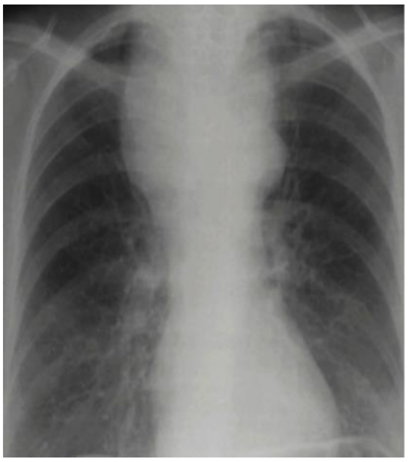

Figure 2. Suspicion of a mediastinal mass.

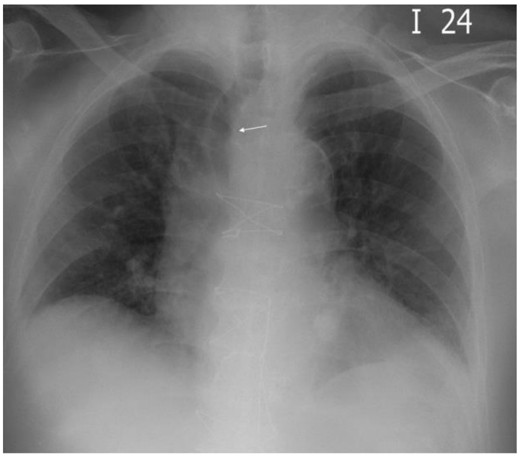

Figure 3. Distortion of anatomy.
Note: Chest X-ray showing intimate effect with mediastinal structures. Distortion of the position of midline structures. Note the deviation of the trachea to the right (arrow).

All mediastinal lesions have individual characteristics, however, some of them may overlap, especially in the chest X-ray, which has a great limitation with respect to the tomography, since it is a single projection, most of the time, only with anteroposterior (**Table 2**).

2. Methodology

A review of mediastinal radiological references was performed, with emphasis on their imaging characteristics and epidemiological context. A detailed literature search was performed in the medical databases available according to "MeSH" terms and specific filters. The articles resulting from this search were analyzed and selected for the review. Representative cases from our institution were used and diagrams were designed to exemplify mediastinal references.

3. Mach effect

The Mach effect represents a phenomenon of enhancement of the borders of mediastinal structures on the radiograph. In this effect, the edges of more radiopaque (white) objects appear more radiolucent (black), creating a false shadow[5]. Thus, a dark (radiolucent) shadow appears around the more radiopaque objects, such as vertebrae and the heart, which are located next to more radiolucent objects, such as lung fields. This effect occurs more frequently adjacent to concave structures such as the heart. The Mach effect permits visualization of paraspinal lines, as the presence of these does not occur because of the interface of the lung with

Table 2. Radiographic features of the mediastinal lesions

Tumor	Mediastinal localization	Radiographic features
Thymoma	Anterior	Lobulated mass with well-defined contours; anterosuperior mediastinum; anterior to the aortic button.
Timolipoma	Anterior	Diffuse mediastinal widening; clear margins with lung; no significant mass effect.
Teratoma	Anterior	Opacity in the anterior mediastinum; calcifications.
Retrosternal goiter	Anterior	Homogeneous, lobulated mass; anterosuperior mediastinum; continuity with cervical structures.
Lipoma	Anterior	Homogeneous lobulated mass in the anterosuperior mediastinum.
Germ cell tumors	Anterior	Lobular or round mass; well defined; may be calcified (bones or teeth); large-volume lobulated mass (seminoma).
Bronchogenic cyst	Middle	Mass round, well defined, homogeneous; radiolucent density or solid appearance.
Extension of bronchogenic tumors	Middle	Lymphadenomegaly; mediastinal widening; heterogeneous, lobulated mass with poorly defined borders; mass or nodule in the lung parenchyma.
Lymphoma	Anterior and middle	Adenomegaly
Neurogenic tumors	Posterior	Spherical lesions, very well defined; adjacent to the vertebral bodies; erosion of adjacent ribs; erosion of the conjugation foramina or vertebrae; obliteration of the paraspinal lines.
Aortic aneurysm	Posterior	Posterior mass in continuity with the aortic arch; atheromatous curvilinear calcifications.
Vertebral infections	Posterior	In early stages there may be no findings; osteolytic destruction of the vertebra; anterior vertebral collapse; prominence of prevertebral soft tissues.
Extramedullary hematopoiesis	Posterior	Masses of well-defined, delineated margins; trabeculated costal arches and flared ribs; most frequently in inferior costal arches.
Meningocele	Posterior	Well-defined paravertebral opacities; well-defined or lobulated margins.
Prevertebral hematomas	Posterior	Erasure of the paraspinal lines; there may or may not be mediastinal widening; increased interpeduncular line; vertebral fracture/injury.
Neuroenteric cysts	Posterior	Homogeneous hyperdense lesion with well-defined margins; they may be associated with vertebral lesions at a different level.
Sarcomas	Posterior	Large, ill-defined masses; bone erosions.

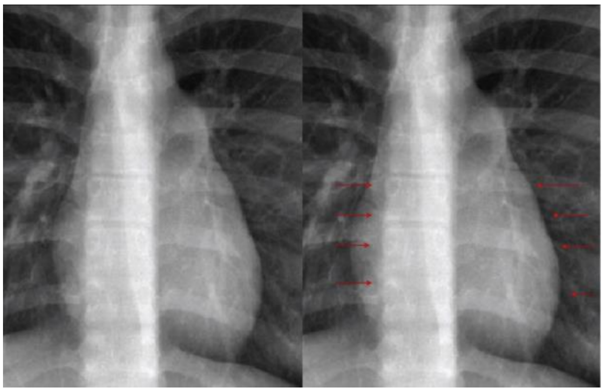

Figure 4. Mach effect.

paraspinal tissues, since the vertebral bodies are more radiopaque than the adjacent lung fields[6] (**Figure 4**). The Mach effect also explains pseudo-pneumomediastinum, which is the false impression of pneumomediastinum around the cardiac silhouette[7].

4. Mediastinal compartments and anatomy

The mediastinal anatomy can be divided into parts based on its relationship to the fibrous pericardium. The superior mediastinum lies above the superior level of the pericardium and Ludwig's plane, which is defined as a horizontal line running from the manubriosternal joint to the inferior vertebral plate of T4[8]. The inferior mediastinum lies below Ludwig's plane. The anterior mediastinum is the compartment anterior to the pericardium. The middle mediastinum lies within the pericardium and the posterior mediastinum is the compartment posterior to the pericardium (**Table 3**). Each of the mediastinal compartments contains its own structures, which are susceptible to alterations.

Table 3. Mediastinal anatomical division with its boundaries and the structures they contain

Division	Limits	Normal structures
Anterior	Anterior: sternum; Posterior: anterior margin of the pericardium, aorta and brachiocephalic vessels.	Timo Lymph nodes Grease Internal mammary vessels
Middle	Anterior: posterior margin of the anterior division; Posterior: anterior margin of the posterior division	Heart and pericardium Ascending and transverse aorta Brachiocephalic vessels Superior and inferior vena cava Main pulmonary vessels Trachea and main bronchi Lymph nodes Grease
Posterior	Anterior: posterior border of the pericardium. Posterior: prevertebral fascia and anterior longitudinal ligament. * The lateral margins of all pulmonary compartments are the parietal pleurae.	Descending aorta Esophage Thoracic duct Acygos or hemiazygos vein Autonomous nerves Lymph nodes Grease

There are different radiologic classifications for dividing the mediastinal compartments, each with discrete variations in the boundaries between them. The most commonly used classifications are the three- and four-compartment models. There are the Felson model, which is the same as the Zylak classification[9], the Fraser and Paré model[10], the Burkell classification[11], the model proposed by the Japanese Association for Thymus Research (JART)[11] and the anatomic model. The JART model and the anatomic classification divide the mediastinum into four compartments, whereas the Felson and Burkell classification divide it into three. Recently, an alternative classification, called ITMIG (International Thymic Malignancy Interest Group), has been proposed based on computed tomography cross-sectional images; however, its review is beyond the scope of this article[12].

The three-compartment model (Felson model) is the one that will be used throughout this review because it allows for the simplest approach to chest radiography (**Figure 5**).

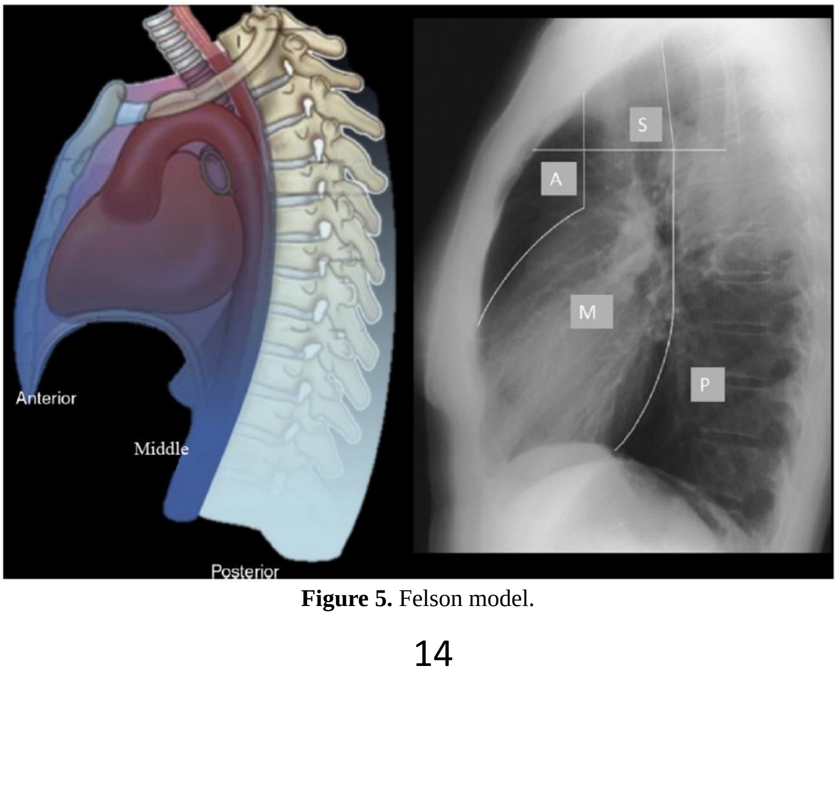

Figure 5. Felson model.

The Felson model, which is the same as the Zylak classification, uses the lateral chest radiograph as a reference. The anterior and middle mediastinum are separated by a line extending along the dorsum of the heart silhouette and the anterior aspect of the trachea. The posterior mediastinum lies between the posterior line of the trachea and a line located 1 cm posterior to the anterior margin of the vertebral bodies.

5. Semiology of the mediastinum according to its lines, bands and interfaces

The radiological references of the mediastinal anatomy in chest radiography are lines, bands and interfaces.

A line is a longitudinal opacity no more than 1–2 mm wide. These are the anterior and posterior pleural junction lines and the right and left paraspinal lines. They are formed from the close apposition of the parietal and visceral pleura of both lungs, in the case of the junction lines, or from the apposition of the two layers of the pleura to the lateral margins of the vertebral bodies, in the case of the paraspinal lines. The latter can also be explained by the Mach effect.

A band is a longitudinal opacity 2–5 mm wide. In the mediastinum they correspond to paratracheal bands. They are formed by the apposition of the parietal pleurae of the upper lobes with the lateral walls of the trachea.

An interface is formed by the apposition of two tissues of different densities, such as the lungs and the heart. The azygoesophageal interface and the descending aorta interface are the most important anatomical landmarks.

Displacement of a mediastinal line, widening of a band or abnormal contour of an interface are important signs of mediastinal pathology (**Figure 6**).

The mach effect is an optical effect between areas of slightly different density. It can mimic a pneumo-mediastinum. These images show the right paraspinal line and the left cardiac silhouette, both of which are mach lines.

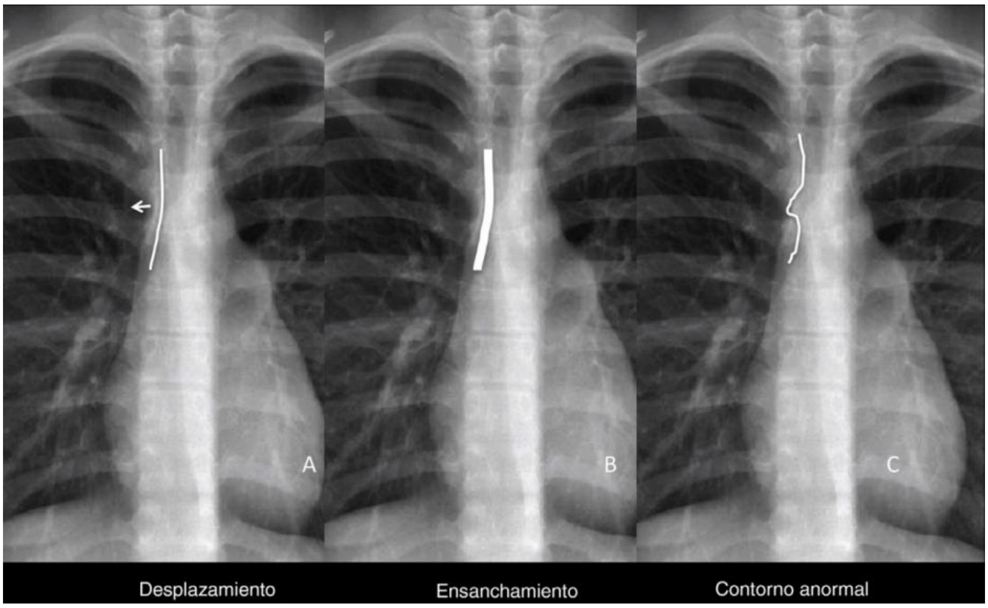

Figure 6. Diagrams representing alterations in the right paratracheal band.
Note: A—displacement; B—widening; C—abnormal contour. These changes are important signs of mediastinal pathology.

6. Anterior mediastinum

Alterations of the anterior mediastinum are usually visualized as alteration of the anterior junction line, the presence of the hilum overlap sign and, in the case of a mass, its continuity with the diaphragm and the absence of its interface with the lung (**Table 4**).

6.1 Alteration of the anterior junction line

This line is located posterior to the sternum, in its upper two thirds and has an oblique orientation from right to left and cephalic to caudal.

It is visualized in 24 to 50% of chest radiographs and is more easily seen in patients with pneumothorax or with emphysema due to lung hyperaeration (**Figure 7**). It may disappear or thicken focally or diffusely due to the presence of anterior mediastinal masses. Its contours may be altered by lesions specific to the anterior mediastinum such as endothoracic goiter, thymoma and mediastinitis[3].

In the adult, anterior mediastinal masses present the highest risk of malignancy. Approximately 56% of all anterior mediastinal lesions are malignant[13,14]. The most frequent masses in the anterior mediastinum are thymic and thyroid gland masses. These masses alter the contour of the anterior junctional lines (**Figure 8**).

The Felson model (left), is a radiologic classification and divides the mediastinum into 3 compartments. This model uses the lateral chest radiograph as a reference. In the classification on the right, different from the Felson model, there is superior and inferior mediastinum.

Table 4. Signs of anterior mediastinal disruption

Alteration of the previous union line
Hilum superposition sign
Cervicothoracic sign
Silhouette sign
Sign of hilar convergence

6.2 Sign of overlapping hilum

It is useful to distinguish a hilar mass from a non-hilar mass. It allows to locate a mass in the anterior or posterior mediastinum. If the hilar vessels can be visualized through the mass, it means that the mass does not arise from the hilum and therefore will be located in the anterior or posterior mediastinum. Most of these masses will be located in the anterior mediastinum[15] (**Figure 9**).

6.3 Cervicothoracic sign

The anterior mediastinum ends at the superior aspect of the clavicles and the posterior mediastinum ends above the level of the clavicles. When a mass projects above the clavicles, it is most likely located in the middle or posterior mediastinum or neck[16]. Additionally, supraclavicular masses that are not located within the mediastinum do not have a clear interface with the lung and their margins are not well defined, contrary to supraclavicular mediastinal masses located in the middle or posterior mediastinum (**Figure 10**).

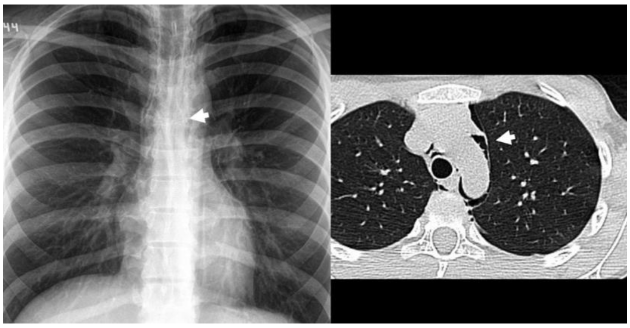

Figure 7. Increased visualization of the anterior line.
Note: History of closed cervicothoracic trauma. Chest radiograph shows signs of pneumomediastinum and subcutaneous emphysema in supraclavicular region. The anterior junctional line related to pneumomediastinum (arrow) can be more easily identified.

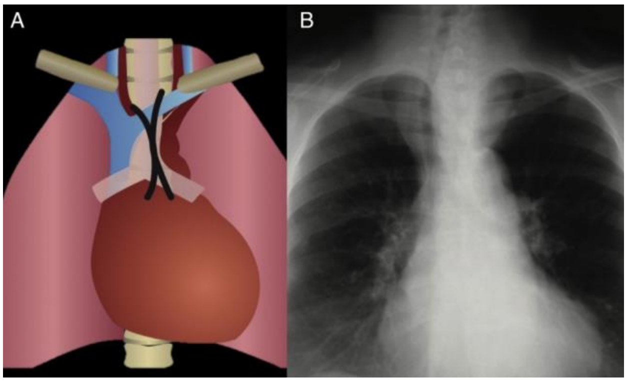

Figure 8. Anterior junction line distortion. **(A)** Scheme showing the location of the normal anterior attachment line; **(B)** mass in the upper third of the anterior mediastinum with effacement of the anterior junction line, displacement of the trachea to the right and clear interface with the lung, representing a mediastinal mass. The patient is diagnosed with endothoracic goiter.

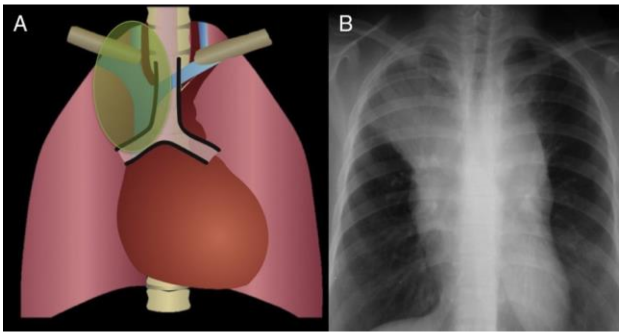

Figure 9 Hilum overlap sign. **(A)** Diagram showing the parahilar lines; **(B)** chest radiograph showing a mass with well defined borders located in the upper third of the mediastinum, hilum overlap sign and disappearance of the anterior junctional line. The patient was diagnosed with thymic carcinoma. The hilum overlap sign can help in the differentiation of anterior or posterior mediastinal masses from masses of the middle mediastinum. Anterior or posterior mediastinal masses overlap the hilum without displacing it.

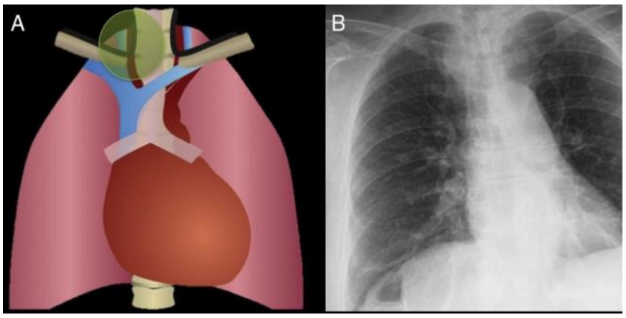

Figure 10. Posterior mediastinal mass.
Note: Mediastinal mass projecting over the right clavicle, with clear interface with the lung and well-defined margins. Endothoracic goiter was confirmed. When a mass projects above the clavicles, it is likely located in the posterior mediastinum or cervical structures.

6.4 Silhouette sign

This sign consists of the loss of the borders of the structures of the same density that are in contact. Masses of the anterior mediastinum in contact with the anterior border of the diaphragm or the pericardium will have poorly distinguishable borders. Therefore, anterior mediastinal masses usually present the silhouette sign. In anterior mediastinal pathology, lesions presenting this sign include lipomas, pericardial cysts, and Morgagni’s hernias (**Figure 11**).

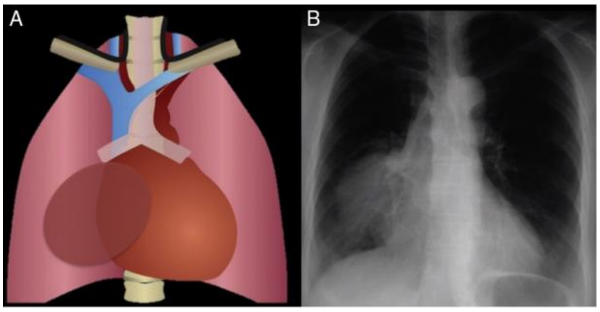

Figure 11. Silhouette sign.
Note: Right parahilar homogeneous mass, with well defined borders, in contact with the diaphragm and making silhouette sign with the mediastinum in a patient with thymus carcinoma.

6.5 Middle mediastinum

Lesions of the middle mediastinum may manifest as obliteration of the aorto-pulmonary window or widening of the paratracheal bands. The presence of lymphadenomegaly and mediastinal widening are other findings that also point to alterations of the middle mediastinum (**Table 5**).

Table 5. Signs of mediastinal disruption

Aorto-pulmonary window obliteration
Widening of the paratracheal bands
Mediastinal widening
Lymphadenomegaly
Tracheal deviation
Alteration in the left subclavian interface

6.6 Aorto-pulmonary window obliteration

The aorto-pulmonary window is the concavity formed between the aortic arch and the left pulmonary artery. It is delimited laterally by the parietal pleura and medially by the ligamentum arteriosum. Its normal appearance is a concavity. It is a visible anatomical landmark on most chest radiographs. It may become convex in the presence of lymphadenopathy, enlargement of the ductus arteriosus and aortic aneurysms. Compartment mediastinal masses, nerve sheath tumors of the left recurrent laryngeal nerve and vagus nerve may also alter the contour of the aorto-pulmonary window (**Figure 12**).

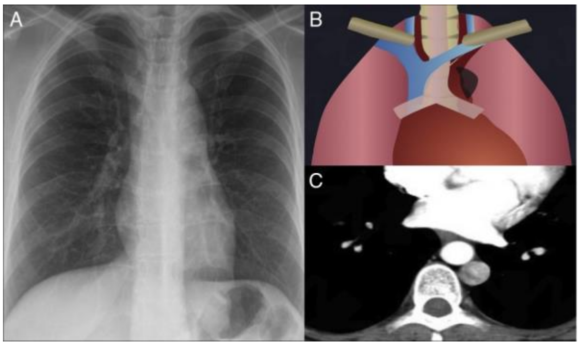

Figure 12. Aortopulmonary window. Chest radiograph **(A)** and illustration **(B)** showing the convex contour of the aortopulmonary window, which is considered abnormal. CT scan **(C)** reveals the presence of the left superior vena cava as an anatomical variant. Mediastinal masses of the anterior compartment or nerve sheath tumors of the recurrent laryngeal nerve and left vagus nerve may also alter the contour of the aortopulmonary window.

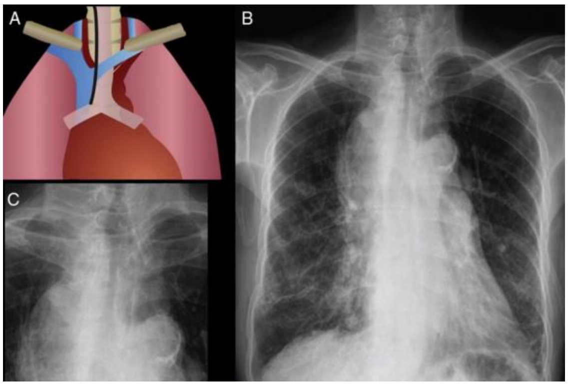

Figure 13. Right paratracheal band.
Note: Thickening of both paratracheal bands, predominantly the right band, suggestive of middle mediastinal disease. Associated paratracheal lymphadenopathy was identified. Small cell lung carcinoma was confirmed.

In the presence of diaphragmatic paralysis or paralysis of the left vocal cord, the aortopulmonary window should be evaluated to rule out tumor lesions of the laryngeal nerve and vagus nerve[1,2,17].

6.7 Widening of the right paratracheal band

It is one of the most frequently visualized anatomical landmarks in chest radiographs, and is present in up to 97% of chest radiographs[15]. The right paratracheal band is 1–4 mm thick, formed by the tracheal wall, mediastinal tissue and adjacent pleura of the right lung; it also has a close relationship with the azygos vein (**Figure 13**).

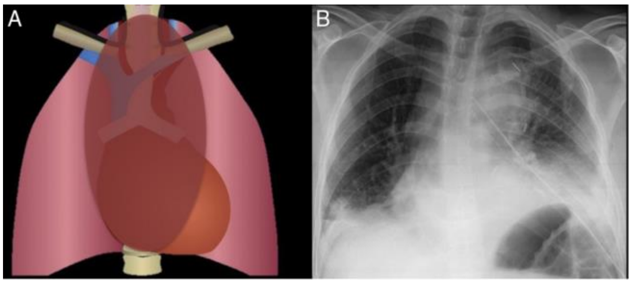

Figure 14. Mediastinal widening.
Note: Thickening of the paratracheal bands, predominantly right band, suggestive of middle mediastinal disease. Associated paratracheal lymphadenopathy. Small cell lung carcinoma is confirmed.

Thickening of the paratracheal band may be due to mediastinal lipomatosis, lymphadenomegaly, tracheal masses or mediastinal hematomas. In the presence of a history of trauma, a right paratracheal band of normal thickness decreases the possibility of mediastinal hematoma and injury to large vessels[18].

6.8 Left paratracheal line

It is formed from the contact between the left lung, the left tracheal wall and the adjacent soft tissues; it is located over the aortic arch, under the upper thoracic arch. It can be a line or a band and its visualization is uncommon, being appreciable in only 21 to 31% of radiographs[2,19,20]; for this reason, its widening can be difficult to see in chest radiographs.

Similar to the right paratracheal band, the presence of osteofits, medistinal lipomatosis, or hemorrhage may alter its appearance. Tortuosity of the aorta may displace this band.

6.9 Mediastinal widening

It is defined as an increase in the transverse diameter of the mediastinum of more than 8 cm measured at the height of the aortic arch[21]. It is one of the most frequent signs of mediastinal disease, occurring in approximately 77% of patients with mediastinal lesions[14] (**Figure 14**).

Some authors consider that the best way to estimate mediastinal widening (**Figure 15**) is the “left mediastinal width”, which is a measurement taken from the midline of the trachea to the left lateral border of the mediastinum at the level of the aortic arch. Its standard values are 5 to 5.5 cm. The widening of the “left mediastinal width” and of the vascular pedicle can also occur when there is dilatation of the great vessels, lymphadenomegaly, mediastinal masses or pleural alterations[16,19].

When the cutoff values of 7.3–9.4 cm are used, the specificity for the detection of mediastinal pathologies is high. The sensitivity of this observation increases when the left mediastinal width is used[22].

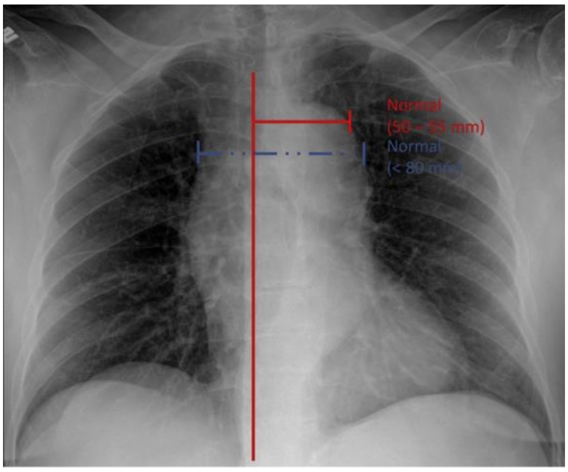

Figure 15. Mediastinal width measurement.
Note: Measurement of traditional mediastinal width (blue lines) and left mediastinal width (red lines).

6.10 Lymphadenomegaly

They are a frequent finding in many mediastinal diseases and their differential diagnosis is broad. A high percentage of the diseases that affect the mediastinum have lymphadenomegaly as a form of presentation, which may or may not be associated with mediastinal widening[23]. Lymphadenomegalies are the most frequent form of presentation of primary mediastinal lymphoma, mediastinal extension of lymphoma and mediastinal compromissory for bronchogenic carcinoma[24] (**Figure 16**).

The sensitivity and specificity of chest radiography has a moderate performance for the detection of adenomegaly, 67% and 59% respectively. Performing anteroposterior and lateral projections of the chest together does not increase the detection of adenomegaly[25].

Lymphadenomegaly in lymphoma, sarcoidosis and cystic fibrosis is a frequent finding. In the latter they are chronic, do not resolve over time and are associated with greater pulmonary involvement[26].

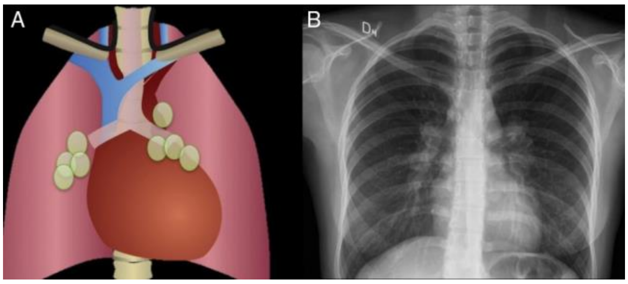

Figure 16. Lymphadenomegaly. **(A)** Schematic and **(B)** radiograph showing thickening of both paratracheal lines by multiple lymphadenopathies compromising the middle mediastinum. Sarcoidosis was confirmed.

6.11 Tracheal deviation

It is a very useful sign in the detection of mediastinal alterations and it is a finding that indicates an alteration of the middle mediastinum. In the elderly patient, there is a fisiological deviation to the right of the lower third of the trachea secondary to flattening of the aortic arch and should not be confused with a disease[15]. Tracheal deviation can also be a normal finding in the pediatric population[27].

It is also an incidental finding in up to 37% of patients. In practice, this finding does not correlate with dificulty in intubation or an increase in the number of intubation attempts in these patients[27,28].

In the context of trauma, alterations in chest radiography allow us to suspect tracheal injury; however, it has greater sensitivity to detect lesions of the pulmonary hilum than lesions of the trachea[29]. Chest radiographic findings suggestive of tracheal injury include subcutaneous cervical emphysema, pneumomediastinum, pneumothorax, and visualization of air around a bronchus (**Figure 7**). Tracheal injury should also be suspected in clavicular (proximal third), scapular, sternal, or costal (first and second arch) fractures[28,30,31].

Despite being a prominent radiological finding, tracheal deviation is more associated with benign diseases, such as intrathoracic goiter[32]. In malignant diseases, tracheal deviation is associated with lymphadenomegaly[33].

Thyroid masses often influence the position and dimensions of the trachea because of the proximity of the thyroid to the tracheal wall and the fact that the thyroid capsule is intertwined with the connective tissue surrounding the trachea[34] (**Figure 17**).

6.12 Alteration in the interface of the left subclavian artery

It is the interface formed between the pleura of the left lung, the left subclavian artery and the adjacent mediastinal fat. This mediastinal reference can be visualized and altered in the presence of lymphadenomegaly, tortuosity of the subclavian artery or pleural alterations.

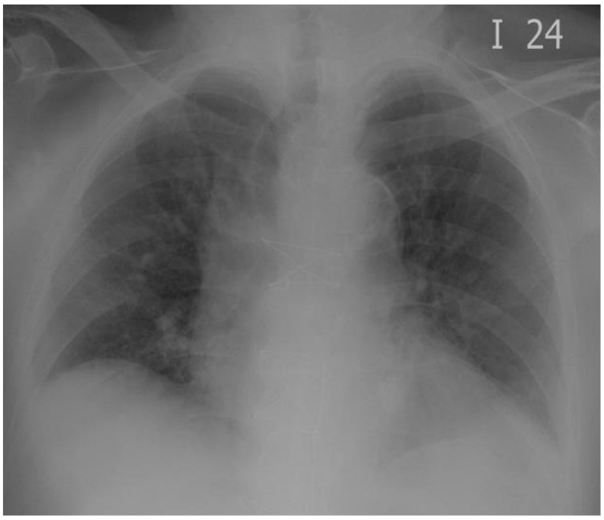

Figure 17. Tracheal deviation.
Note: Significant deviation of the trachea to the right, secondary to aneurysm of the ascending aorta. Bilateral alveolar opacities due to multilobar pneumonia.

7. Posterior mediastinum

7.1 Distortion of paraspinal lines

The paraspinal lines, also called paravertebral lines, are formed from the interface between the medial portions of the pleura of the posterior lobes and the paravertebral tissues of the spine (**Figure 18**). They are abnormal when there is thickening, displacement, or disruption in their continuum (**Table 6**).

The left paraspinal line lies below the aortic arch and extends vertically to the left diaphragmatic crura parallel to the spine, in the middle of the spine and the lateral margin of the aorta. The right paraspinal line is thinner than the left paraspinal line and therefore less visible. The right paraspinal line is best visualized in its portion adjacent to the inferior vertebrae of the thoracic spine, where it converges vertically toward the right diaphragmatic crura. In its superior portion, it is visualized adjacent to the air column of the trachea[19].

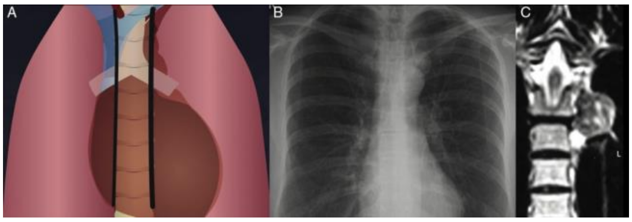

Figure 18. Paraspinal lines. Illustration **(A)** of the normal paraspinal lines. Chest radiograph **(B)** demonstrates a well defined mass in the upper third of the left mediastinum, projecting over the aortic arch, originating from the left paraspinal line. Coronal MRI with T2 information **(C)** shows the same left paravertebral mass, which has heterogeneous signal intensity in a patient with extramedullary hematopoiesis. Visualization of the left paraspinal line is more frequent than the right line.

Table 6. Posterior mediastinal landmarks

Distortion of the paraspinal lines
Distortion of the para-aortic line
Obliteration of the posterior junction line
Distortion of the azygoesophageal recess

The left paravertebral line is usually ed by processes that affect the diameter and course of the thoracic aorta. The most frequent cause of thickening of the right paravertebral line is osteophytes[19]. The pathologies that can affect both paravertebral lines are vertebral trauma, pleural effusion, adenomegaly, vertebral and paravertebral alterations, posterior paravertebral masses and widening of the azygos and hemiazygos veins.

In the context of trauma, injuries to the thoracic vertebrae, particularly the upper thoracic vertebrae, are detected from altered paraspinous lines and are accompanied by other major traumatic injuries in 83% of cases[35] (**Figure 19**). In general, the upper thoracic vertebrae are more difficult to visualize than the rest of the vertebral segments given the interposition of the shoulders, the three upper ribs and the increased density of the upper mediastinum. For this reason, the detection of other findings suggestive of traumatic vertebral lesions is very useful. These findings include displacement of the vertebral bodies, spinous processes and nasogastric tube, as well as loss of vertebral body height, alteration in the shape of the articular facets and mediastinal flaring[36].

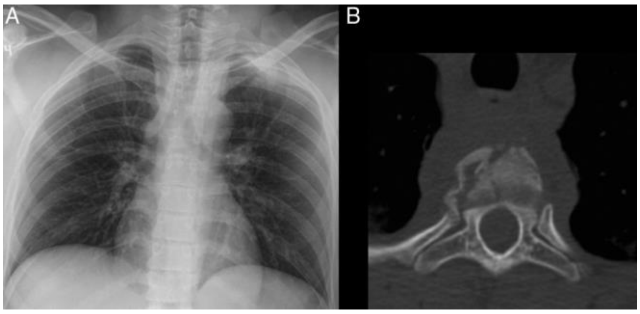

Figure 19. Vertebral fracture and relationship with paraspinal lines. 23-year-old patient with a history of trauma. **(A)** Chest X-ray showing widening of the paraspinal lines in the upper third of the thorax without a clear decrease or alteration of the vertebral bodies. Chest CT scan **(B)** shows an impacted fracture of the T3 vertebral body with prominence of prevertebral and paravertebral tissue corresponding to hematoma.

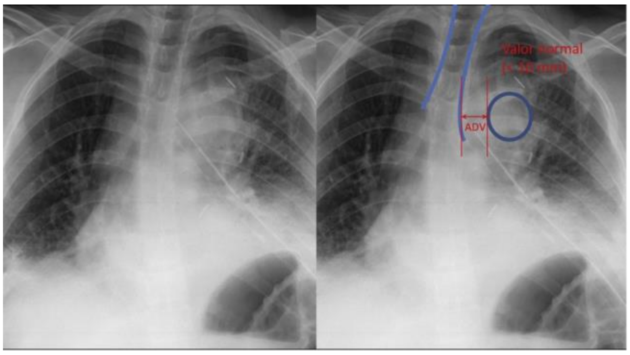

Figure 20. Aortic button displacement.
Note: Aortic knob displacement on chest radiograph; we draw a circle along the aortic knob. The magnitude of the aortic displacement is measured as the distance between the medial edge of the circle and the left margin of the tracheal air column. In this patient, an ADV (aortic displacement value) greater than 10 mm is observed. Mediastinal hemorrhage was confirmed.

7.2 Para-aortic line distortion

It is a line that is best visualized in the lateral projection. This line is produced by the contact between the descending aorta and the medial aspect of the left lower lobe and is observed below the aortic arch, parallel to the left paravertebral line. Its visualization in chest radiographs is frequent. It can be accentuated in cases of dorsal hyperkyphosis, tortuosity of the aorta and pulmonary enfisema[15].

Displacement of the aortic arch from the mid-aortic circumference to the left margin of the trachea is more than 10 mm, and it has moderate sensitivity and specification, 78% for each, in the diagnosis of a left paratracheal esophageal mediastinal paratracheal mass[36] (**Figure 20**).

Obliteration of the para-aortic line can occur without necessarily representing a pathological condition[37] and can be explained by the apposition of any of the hilar structures, including the left pulmonary vein, mediastinal fat and left ventricle.

Increased convexity is related to tortuosity or dilatation of the aorta. Occasionally, focal convexities of the para-aortic line can be observed, which may correspond to aortic aneurysms, adenomegaly, paraspinal masses or neurogenic tumors[15].

7.3 Obliteration of the posterior junction line

It is formed by the apposition of the pleura and a varying amount of fat in the superior mediastinum, posterior to the esophagus and anterior to the upper thoracic vertebral bodies. It is usually a straight or slightly concave line directed caudally that always ends at the superior border of the aortic arch. A mediastinal landmark is commonly visualized and can be altered in the presence of esophageal disease or masses[19] (**Figure 21**).

7.4 Distortion of the azygo-esophageal recess

The azygos-esophageal recess is a mediastinal interface created by the space between the lateral wall of the middle and lower third of the esophagus and the pulmonary pleurae anterior to the spine. It extends from the arch of the azygos vein to the aortic hiatus[2]. The azygos-esophageal line is visualized as an "inverted S". It has a slight convexity to the left in the superior segment with a straight inferior border. Right superior convexity can be seen in children and young adults, but is abnormal in older adults[2,38]. It may present with concave morphology in 21% of patients without this representing alterations[39] (**Figure 22**).

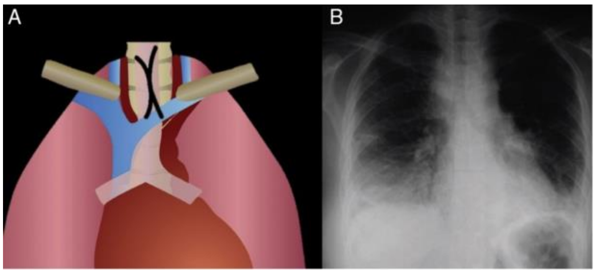

Figure 21. Obliteration of the posterior junction line. **(A)** Schematic showing the posterior junction line. **(B)** Mediastinal widening, bilateral pleural effusions and absence of posterior junction line in a patient with retropharyngeal mediastinitis abscess.

Figure 22. Esophageal azygos recess distortion.
Note: Rectification and deviation of the posterior esophageal azygos esophageal recess related to mediastinitis and mediastinal abscess.

Displacement of the azygo-esophageal line may arise from partial or complete lower lobe atelectasis, esophageal dilatation and posterior mediastinal masses[38]. An abnormal contour of this line may be due to lymphadenopathy, hiatal hernias, bronchopulmonary malformations, esophageal neoplasms, pleural abnormalities and cardiomegaly with dilatation of the left atrium[2].

8. Mediastinum in lateral projection

8.1 Posterior tracheal line

It is formed by the apposition of the posterior wall of the trachea, soft tissues and pleura of the right lung, and has a normal thickness of 2.5 mm. In some patients, it may be thicker and reach up to 5.5 mm. In that case, it is referred to as a posterior tracheal band and is a finding explained by the interface of the posterior wall of the trachea with the anterior wall of the esophagus, rather than the right lung[40] (**Figure 23**).

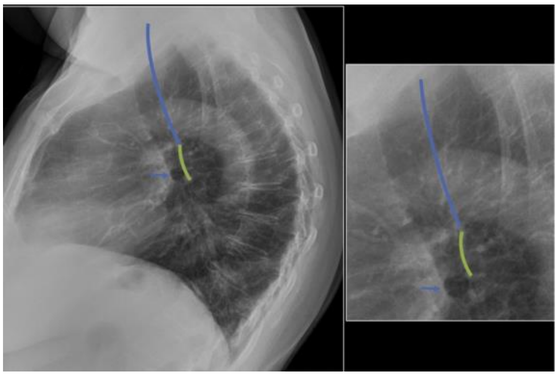

Figure 23. Lateral X-ray of the hilar anatomy.
Note: Lateral radiograph showing partial hilar anatomy. The posterior wall of the trachea (blue line) is visible superiorly. The right upper lobe bronchus (blue arrow) can be seen as an oval lucency within the superior hilar shadow. Below the posterior wall of the trachea, the posterior wall of the intermediate bronchus (green line) is visible at the level of its bifurcation.

8.2 Posterior wall of the bronchus intermedius

It is a vertical line corresponding in its upper portion to the posterior wall of the right main bronchus and in its lower portion to the posterior wall of the bronchus intermedius[40,41] (**Figure 23**).

The posterior wall of the bronchus intermedius normally has a thickness of 0.5–2 mm and is considered an abnormal thickening when it is above 3 mm.

Its maximum length is 50 mm. It only achieves adequate delineation in 55% of patients[41-43] (**Figure 23**).

9. Conclusions

Mediastinal lesions usually present in a nonspecific manner. Despite advances in biopsy techniques and imaging, histologic examination is required to establish a diagnosis and rule out malignancy.

Traditionally, anatomical references such as lines, bands and interfaces have been mentioned, which are useful in the identification of mediastinal lesions. However, to date, these references have variable visualization percentages and do not achieve a sufficiently high sensitivity to guide towards an accurate etiological diagnosis of a mediastinal mass; however, there are much more sensitive features to alert about the presence of mediastinal lesions such as mediastinal widening and adenomegaly.

With a careful approach to mediastinal lesions based on radiological semiology and emphasis on the prevalence of mediastinal lesions in each compartment, differential diagnoses can be narrowed.

Acknowledgments

We here express our gratitude to the entire thoracic radiology team of the University Hospital of the Fundación Santa Fe de Bogotá.

Conflict of interest

The authors declare that they have no conflict of interest.

References

1. Proto AV. Mediastinal anatomy: Emphasis on conventional images with anatomic and computed tomographic correlations. Journal of Thoracic Imaging 1987; 2: 1–48.
2. Gibbs JM, Chandrasekhar CA, Ferguson EC, *et al*. Lines and stripes: Where did they go—From Conventional Radiography to CT. RadioGraphics 2007; 27: 33–48.
3. Heitzman ER. The mediastinum: Radiologic correlations with anatomy and pathology. 2nd ed. Berlin: Springer; 2012. p. 355.
4. Dobson MJ, Carrington BM, Parsons VJ, *et al*. What is the value of the lateral chest radio- graph in the follow-up thoracic lymphoma? European Radiology 1997; 7: 1110–1113.
5. Panikkath R, Panikkath D. Mach band sign: An optical illusion. Baylor University Medical Center Proceedings 2014; 27: 364–365.
6. Chasen MH. Practical applications of Mach band theory in thoracic analysis. Radiology 2001; 219: 596–610.
7. Gunn ML (editor). Pearls and pitfalls in emergency radiology: Variants and other difficult diagnoses [Internet]. 2013. Available from: https://www.amazon.com/Pearls-Pitfalls-Emergency-Radiology-Difficult/dp/110702191X.
8. Sinnatamby C. Last's anatomy: Regional and applied. Australia: Elsevier; 2003.
9. Zylak CJ, Pallie W, Pirani M, *et al*. Anatomy and computed tomography. RadioGraphics 1983; 3: 478–530.
10. Fraser RS, Müller NL, Colman N, *et al*. Fraser and Paré's diagnosis of diseases of the chest [Internet]. 1999. Available from: https://www.cabdirect.org/cabdirect/abstract/20002009269.
11. Fujimoto K, Hara M, Tomiyama N, *et al*. Proposal for a new mediastinal compartment classification of transverse plane images according to the Japanese Association for Research on the Thymus (JART) General Rules for the Study of Mediastinal Tumors. Oncology Reports 2014; 31: 565–572.
12. Carter BW, Tomiyama N, Bhora FY, *et al*. A modern definition of mediastinal compartments. Journal of Thoracic Oncology 2014; 9: S97–S101.
13. Takeda S, Miyoshi S, Akashi A, *et al*. Clinical spectrum of primary mediastinal tumors: A comparison of adult and pediatric populations at a single Japanese institution. Journal of Surgical Oncology 2003; 83: 24–30.
14. Aroor AR. A study of clinical characteristics of mediastinal mass. Journal of Clinical and Diagnostic Research 2014; 8(2): 77–80.
15. Coche EE, Ghaye B, Mey JD, *et al*. Comparative interpretation of CT and standard radiography of the chest. Secaucus: Springer Science & Business Media; 2011.
16. Giron J, Fajadet P, Sans N, *et al*. Diagnostic approach to mediastinal masses. European Journal of

Radiology 1998; 27: 21–42.
17. McComb BL. Reflecting upon the left superior mediastinum. Journal of Thoracic Imaging 2001; 16: 56–64.
18. Wright FW. Radiology of the chest and related conditions. Boca Raton: CRC Press; 2001.
19. Webb WR, Higgins CB. Thoracic imaging: Pulmonary and cardiovascular radiology. Philadelphia: Lippincott Williams & Wilkins; 2010.
20. Hansell DM. Imaging of diseases of the chest: Expert consult—Online and print. 5th ed. Edinburgh: Mosby; 2009.
21. Lai V, Tsang WK, Chan WC, *et al*. Diagnostic accuracy of mediastinal width measurement on posteroanterior and anteroposterior chest radiographs in the depiction of acute nontraumatic thoracic aortic dissection. Emergency Radiology 2012; 19: 309–315.
22. Lai V, Tsang WK, Chan WC, *et al*. Diagnostic accuracy of mediastinal width measurement on posteroanterior and anteroposterior chest radiographs in the depiction of acute nontraumatic thoracic aortic dissection. Emergency Radiology 2012; 19: 309–315.
23. Naidich DP, Müller NL, Webb WR. Computed tomography and magnetic resonance of the thorax. Philadelphia: Lippincott Williams & Wilkins; 2007.
24. Suwatanapongched T, Gierada DS. CT of thoracic lymph nodes. Part II: Diseases and pitfalls. British Journal of Radiology 2006; 79: 999–1000.
25. Swingler G, du Toit G, Andronikou S, *et al*. Diagnostic accuracy of chest radiography in detecting mediastinal lymphadenopathy in suspected pulmonary tuberculosis. Archives of Disease in Childhood 2005; 90: 1153–1156.
26. Don CJ, Dales RE, Desmarais RL, *et al*. The radiographic prevalence of hilar and mediastinal adenopathy in adult cystic fibrosis. Canadian Association of Radiologists Journal 1997; 48: 265–269.
27. Costa NS, Laor T, Donnelly LF. Superior cervical extension of the thymus: A normal finding that should not be mistaken for a mass. Radiology 2010; 256: 238–242.
28. Kar P, Rath GP, Prabhakar H, *et al*. Tracheal deviation may be a normal anatomical variant in children. Anaesthesia and Intensive Care 2009; 37: 144–145.
29. Scaglione M, Romano S, Pinto A, *et al*. Acute tracheobronchial injuries: Impact of imaging on diagnosis and management implications. European Journal of Radiology 2006; 59: 336–343.
30. Unger JM, Schuchmann GG, Grossman JE, *et al*. Tears of the trachea and main bronchi caused by blunt trauma: Radiologic findings. American Journal of Roentgenology 1989; 153: 1175–1180.
31. Hong BW, Mazeh H, Chen H, *et al*. Routine Chest X-ray prior to thyroid surgery: Is it always necessary? World Journal of Surgery 2012; 36: 2584–2589.
32. Adegboye VO, Brimmo AI, Adebo OA, *et al*. The place of clinical features and standard chest radiography in evaluation of mediastinal masses. West African Journal of Medicine 2003; 22: 156–160.
33. Díez JJ. Goiter in adult patients aged 55 years and older: Etiology and clinical features in 634 patients. The Journals of Gerontology: Series A 2005; 60: 920–923.
34. Buckley JA, Stark P. Intrathoracic mediastinal thyroid goiter: Imaging manifestations. American Journal of Roentgenology 1999; 173: 471–475.
35. Van Beek EJR, Been HD, Ponsen K-J, Maas M. Upper thoracic spinal fractures in trauma patients—A diagnostic pitfall. Injury 2000; 31: 219–223.
36. Yang DH, Seo JB, Lee IS, *et al*. Displaced aortic arch sign on chest radiographs: A new sign for the detection of a left paratracheal esophageal mass. European Radiology 2004; 15: 936–940.
37. Takahashi K, Shinozaki T, Hyodo H, *et al*. Focal obliteration of the descending aortic interface on normal frontal chest radiographs: Correlation with CT findings. Radiology 1994; 191: 685–690.
38. Marchiori D. Clinical imaging: With skeletal, chest and abdomen pattern differentials. United Kingdom: Elsevier Health Sciences; 2004.
39. Heitzman ER, Groskin SA. The lung: Radiologic-pathologic correlations. 3rd edition. St. Louis: Mosby; 1993.
40. Franquet T, Erasmus JJ, Giménez A, *et al*. The retrotracheal space: Normal anatomic and pathologic appearances. RadioGraphics 2002; 22(S1): 231–246.
41. Webb WR, Hirji M, Gamsu G. Posterior wall of the bronchus intermedius: Radiographic-CT correlation. American Journal of Roentgenology 1984; 142: 907–911.
42. Frija J, de Kerviler E, Zagdanski AM. Radiologic anatomy of the inferior lung margins as demonstrated on computed radiography with enhancement of low frequencies. Surgical and Radiologic Anatomy 1997; 19: 257–263.
43. Biemans JMA, Van Heesewijk JPM, Van Der Graaf Y. Digital chest imaging: Selenium radiography versus storage phosphor imaging. Comparison of visualization of specific anatomic regions of the chest. Investigative Radiology 2002; 37: 47–51.